


## STANDARD ARTICLE OPEN ACCESS

Small Animal Internal Medicine Neurology

# A Dorsal Intramedullary T2-Weighted Hypointense Signal Suggests Haemorrhagic Necrotic Material Indicating Ascending-Descending Myelomalacia in Dogs

Ursula Teubenbacher<sup>1</sup>  | Diana Henke<sup>2</sup> | Anna Oevermann<sup>3</sup> | Daniela Schweizer<sup>1</sup>

<sup>1</sup>Division of Clinical Radiology, Department of Clinical Veterinary Medicine, Vetsuisse Faculty, University of Bern, Bern, Switzerland | <sup>2</sup>Neurological Department, Veterinary Clinic Stuttgart, Stuttgart, Germany | <sup>3</sup>Division of Neurological Sciences, DCR-VPH, Vetsuisse Faculty, University of Bern, Bern, Switzerland

**Correspondence:** Ursula Teubenbacher ([ursula.teubenbacher@uzh.ch](mailto:ursula.teubenbacher@uzh.ch))**Received:** 30 May 2024 | **Revised:** 24 February 2025 | **Accepted:** 25 February 2025**Funding:** The authors received no specific funding for this work.**Keywords:** canine | disc herniation | intramedullary signal changes | magnetic resonance imaging | softening of the spinal cord

## ABSTRACT

**Background:** Ascending-descending myelomalacia (ADMM) is a progressive softening of the spinal cord observed in dogs after spinal cord injury (SCI). On histopathology, areas of hemorrhagic necrotic material are found in the central canal and dorsal funiculi.

**Hypothesis/Objectives:** We investigated if hemorrhagic necrotic material dorsal to the central canal can be identified on magnetic resonance imaging (MRI). We hypothesized that signal changes are seen in dogs with ADMM, but not in those without ADMM.

**Animals:** Twenty-six dogs with pathologically confirmed ADMM, focal myelomalacia (FM) and 10 control dogs.

**Methods:** Retrospective case-control study comparing intramedullary signal dorsal to the central canal in dogs with ADMM, FM, and control dogs.

**Results:** A hypointense signal dorsal to the central canal on transverse T2-weighted fast spin echo and gradient echo images was observed. If present in both T2-d T2\*-weighted sequences, it was significantly associated with ADMM ( $p = 0.004$ ; specificity, 81%; sensitivity, 100%). If the T2-weighted hypointense focus was identified at a distance  $\geq 3$  vertebral bodies from the initial site of spinal cord injury, it was strongly associated with ADMM ( $p = 0.01$ ) with a specificity of 100% and sensitivity of 78%.

**Conclusion and Clinical Importance:** A dorsal intramedullary T2-weighted hypointense focus likely represents hemorrhagic necrotic material in the dorsal funiculi. If present at a distance of  $\geq 3$  vertebral bodies away from the initial site of SCI, it might aid in the diagnosis of ADMM in dogs by MRI.

## 1 | Introduction

Myelomalacia refers to softening of the spinal cord resulting from hemorrhagic or ischemic necrosis. It represents a sequela of spinal

cord injury (SCI), most often secondary to hemorrhagic contusion as seen with intervertebral disc extrusion [1–3]. In dogs with focal myelomalacia (FM), progression is observed over segments neighboring the initial site of injury (“epicenter”), but the spinal cord

**Abbreviations:** ADMM, ascending/descending myelomalacia; CSF, cerebrospinal fluid; FM, focal myelomalacia; FSE, fast spin echo; GRE, gradient echo; HASTE, half-Fourier acquisition single-shot turbo spin echo imaging; IVDH, intervertebral disk herniation; MRI, magnetic resonance imaging; SCI, spinal cord injury; SSTSE, sagittal single-shot turbo spin echo.

This is an open access article under the terms of the [Creative Commons Attribution-NonCommercial-NoDerivs](https://creativecommons.org/licenses/by-nc-nd/4.0/) License, which permits use and distribution in any medium, provided the original work is properly cited, the use is non-commercial and no modifications or adaptations are made.

© 2025 The Author(s). *Journal of Veterinary Internal Medicine* published by Wiley Periodicals LLC on behalf of American College of Veterinary Internal Medicine.

damage remains self-limiting [1]. If areas at least 3 spinal cord segments distant from the epicenter are affected, it is categorized as ascending-descending myelomalacia (ADMM) [2]. In contrast to FM, ADMM is progressive and often fatal. Its pathophysiology has not been fully elucidated, but it has been proposed that the primary impact to the spinal cord and subsequent vascular compromise lead to secondary injury pathways [1, 3–5]. Progression into ADMM is accompanied by rapid neurological deterioration reflecting severe tissue damage depending on spread within the spinal cord [6–11]. The speed of propagation varies from <24 h to weeks [4, 12–14]. Development is described to occur more frequently in dogs that become non-ambulatory in <24 h [6, 12] or if the site of disk extrusion is at L5-6 [12]. In a recent study, however, no significant difference was found regarding the site of disk extrusion [15]. Magnetic resonance imaging (MRI) features suggestive of ADMM are a mildly dilated central canal with irregular margination [8], an intramedullary hyperintense signal on sagittal T2-weighted sequences [12, 16] and attenuations of cerebrospinal fluid (CSF) of  $\geq 7.4$  times the length of L2 on heavily T2-weighted sequences such as half-Fourier acquisition single-shot turbo spin echo imaging (HASTE) [6, 17]. A region of loss of meningeal and venous sinus contrast is a newly described imaging feature [15]. Affected areas also might exhibit diffusely decreased signal intensity on T2\*-weighted gradient echo sequences indicating subdural, subarachnoidal, or intramedullary hemorrhage [9, 18]. However, these MRI findings indicate advanced propagation of ADMM whereas early ante mortem diagnosis still appears to be problematic [8, 16, 17, 19]. On histopathology, hemorrhagic-necrotic material inside or dorsal to the central canal located either on the midline or between the gray and white matter of the dorsal funiculi is pathognomonic for advanced propagation. Propagation through the central canal presumably leads to central canal distention and to rupture at its weakest dorsal aspect, squeezing hemorrhagic-necrotic debris into the dorsal funiculi in adjacent and even remote segments of the spinal cord, creating an irregular pearl necklace pattern in longitudinal sections of the spinal cord [2]. It is hypothesized that the liquefaction of the tissue in combination with increased intramedullary pressure leads to a mixture of hemorrhagic-necrotic debris with CSF that might facilitate longitudinal extension within the central canal [2]. It is unclear if the pathological observation of hemorrhagic-necrotic debris dorsal to the central canal or in between the dorsal funiculi can be identified on MRI. The aims of our retrospective study were to determine if the intramedullary histopathological findings in and dorsal to the central canal in dogs with ADMM are visible on MRI. For this aim, MRI of dogs with histopathologically confirmed ADMM were compared to those in dogs with a histopathologic diagnosis of FM and to dogs with SCI that recovered after decompressive surgery.

## 2 | Materials and Methods

Study subjects were identified from client-owned dogs presented to the Vetsuisse Faculty University of Bern between 2011 and 2016 by electronic medical records and neuropathological database search. During this time period, dogs with a histopathological diagnosis of ADMM or FM were included only if MRI of the spine included at least T2-weighted FSE sequences in sagittal and transverse planes (Philips Panorama HFO; Philips Medical Systems Nederland B.V., Best, the Netherlands). Pathological evaluation was made based

on agreement between a board-certified neuropathologist and a board-certified neurologist (A.O., D.H.). Myelomalacia at the site of injury was classified as FM. If myelomalacia (ascending, descending, bidirectional) was present at least 3 spinal cord segments distant from the epicenter, it was categorized as ADMM [2]. Segments were defined by dorsal roots entering and ventral roots exiting the spinal cord. Histopathologic evaluation included assessment of the presence of necrotic-hemorrhagic debris within the dorsal funiculi at the epicenter as well as in distant sections of the spinal cord [2].

For control dogs, the clinical database was searched backward from 2016 until 10 dogs presented with paraplegia caused by SCI and severe neurological dysfunction with neurological grade V (loss of nociception) or grade IV (non-ambulatory with no loss of nociception) were found. Additional inclusion criteria were an MRI examination of the spine, including a T2\*-weighted gradient echo (GRE) sequence in the transverse plane and recovery after surgical decompression at least to a non-ambulatory status (neurologic grade III). The control cases were selected by the neurologist blinded to the MRI findings.

For all dogs, signalment, time of clinical presentation, results of neurological examination, duration and progression of neurologic signs, time of MRI, and, if performed, time of follow-up MRI, surgery, and necropsy results were recorded.

All MR images were anonymized and reviewed by a board-certified radiologist (D.S.) blinded to the grouping, using a picture and communication system (IMPAX EE R20 XVI SU1, Agfa Healthcare GmbH, Germany).

The MRI evaluation included the location of the SCI (intervertebral disc space), length of attenuation of CSF signal on a single-shot turbo spin echo sequence (reported as ratio to the length of the vertebral body of L2) and the presence or absence of an irregular dorsal delineation of the central canal on sagittal T2-weighted fast-spin echo (FSE) images.

On transverse images, the spinal cord was evaluated for intramedullary signal changes in or dorsal to or both the central canal, and if observed, their location and length in terms of visibility on consecutive transverse images were recorded as the number of consecutive images. If available, this approach was repeated on T2\*-weighted gradient echo (GRE) images and on T1-weighted images. Their distance to the SCI was reported as the number of vertebral bodies.

A signal void on transverse T2\*-weighted GRE images within the spinal cord either on its own or in combination with low signal intensity changes on transverse T2-weighted FSE was considered intramedullary hemorrhage. If no T2\*-weighted GRE sequence was available, marked hypointensity on transverse or sagittal T2-weighted FSE was interpreted as intramedullary hemorrhage.

### 2.1 | Statistical Analysis

The MRI features were compared among dogs with ADMM, FM, and control dogs. Associations of yes/no variables with groups were calculated using a Fisher's exact test. Specificity

and sensitivity of signal changes dorsal to the central canal for ADMM were calculated. For continuous data (distance of signal changes to the epicenter) the Wilcoxon sum rank test was used to calculate differences between groups. Analysis was done using NCSS Statistical Software 2021; NCSS LLC. Kaysville, Utah, USA, [ncss.com/software/ncss](https://ncss.com/software/ncss)). A *P*-value <0.05 was considered significant.

### 3 | Results

#### 3.1 | Case Information

Thirty-six dogs were included in the study population. Of these, 9 were categorized pathologically as ADMM, 17 as FM, and 10 dogs that recovered after decompressive surgery served as a control group. Age, breed, and sex of the study population are shown in Table 1.

In dogs with ADMM, the time between the onset of clinical signs and clinical presentation ranged from 1 to 3 days (median,

1 day; interquartile range [IQR], 1–1.5 days). All ADMM dogs were paraplegic with loss of nociception (grade V) at the time of clinical presentation. Initial MRI examinations were performed 1–3 days after the onset of neurological signs (median, 1 day; IQR, 1–2 days). Four of nine dogs with ADMM underwent surgery on the day of clinical presentation or 1 day later. The remaining 5/9 dogs received conservative medical management when owners declined surgery because of poor prognosis. None of the dogs with ADMM showed any signs of improvement during hospitalization, and all nine dogs were euthanized. The time between MRI and euthanasia ranged from 0 to 11 days (median, 4 days; IQR, 0.5–0.5 days). In two dogs with ADMM, follow-up MRI examination was performed because of a lack of clinical improvement or deterioration 3 and 6 days after the initial MRI, respectively.

In dogs with FM, the time of onset of clinical signs to clinical presentation ranged from ≤24 h to 10 days (median, 1 day; IQR, 0.5–2.5 days). Eleven of seventeen dogs with FM were presented with neurological grade V, 4/17 dogs with grade IV, and 2/17 dogs with grade III (median grade, V). Magnetic resonance imaging was

**TABLE 1** | Breed, number, age and sex of dogs in the ADMM, FM and control group.

Groups	Breeds	Number of dogs	Age [years]			Sex		
			Median	Range	IQR		Male [number of dogs]	Female [number of dogs]
ADMM	Total	9	6	3–14	3–8.5	Total	4	5
	French Bulldog	5				Neutered	2	1
	Mix Breed	3						
	Chinese Crested	1						
FM	Total	17	5.5	2–8	3–7	Total	7	10
	French Bulldog	7				Neutered	4	3
	Mix Breed	2						
	Shi Tzu	2						
	Cocker Spaniel	1						
	Coton de Tulear	1						
	Dachshund	1						
	Labrador Retriever	1						
	Pug	1						
	Tibet Terrier	1						
Control group	Total	10	5.5	3–10	4–7	Total	6	4
	Dachshund	4				Neutered	2	4
	MixBreed	2						
	American Staffordshire Terrier	1						
	Coton de Tulear	1						
	Havanese	1						
	French Bulldog	1						

performed 0–10 days after the onset of neurological signs (median, 1 day; IQR, 1–2.5 days). Six of 17 dogs with FM underwent surgery on the day of clinical presentation or 1 day later. The remaining 11/17 dogs with FM received conservative medical management. Fifteen of 17 dogs were euthanized 1–14 days after hospitalization: 14/15 because of lack of clinical improvement and poor prognosis, and 1/15 at the owner's request despite regaining pain perception and mild motor function. Two of the 17 dogs died spontaneously: one dog neurologically improved after surgery but experienced sudden cardiac arrest 7 days after hospitalization. The other dog died spontaneously after showing marked salivation 5 days after hospitalization. Pathological examination did not identify the cause of death in both dogs. The time between MRI and death ranged from 0 to 12 days. In four dogs with FM, follow-up MRI was performed 1–3 days after the initial MRI.

In control dogs, the time between the onset of clinical signs and clinical presentation ranged from  $\leq 24$  h to  $> 72$  h (median, 1.5 days; IQR, 1–4 days). Eight of ten dogs were presented with neurological grade IV and 2/10 dogs with grade V. Magnetic resonance imaging was performed 1–11 days after the onset of neurological signs (median, 2 days; IQR, 1–4 days). All control dogs underwent surgery 0–2 days after clinical presentation. Time from MRI to release from the hospital ranged from 2 to 17 days (median, 9 days; IQR, 4–10 days). All control dogs recovered to either ambulatory paraparesis (neurologic grade II,  $n=9$ ) or to pain only (neurologic grade I,  $n=1$ ) on follow-up neurological examination. The location of SCI for each group is presented in Table 2.

Findings of dogs with ADMM and FM (signalment, duration of hospitalization, MRI, surgery and histopathology) are illustrated in the [Supporting Information files](#).

### 3.2 | Histopathologic Findings in Dogs With ADMM and FM

In all nine dogs with ADMM, necrotic-hemorrhagic material was present inside the distended central canal or dorsal to the ruptured central canal or both in spinal cord segments distant from the SCI location. If hemorrhagic-necrotic material was present, it was located along the midline and between the gray and white matter of the dorsal funiculi (Figure 1).

In all 17 dogs with a pathological diagnosis of FM, no hemorrhagic-necrotic material was seen dorsally to the ruptured central canal.

### 3.3 | Imaging Findings in Dogs With ADMM, FM and Control Dogs

Magnetic resonance images were available from the location of the suspected SCI; the field of view (FOV) varied with the size of the dog, used coil, and imaging findings. The locations of the SCI for each group are shown in Table 2. The FOV encompassed predominantly the thoracolumbar, lumbar, and lumbosacral spine. The cervical spine also was examined in three dogs with ADMM (one dog during the initial MRI and in two dogs during a follow-up MRI examination). The cervical spinal cord was not

**TABLE 2** | Locations of disc extrusions for dogs with ADMM, FM and control groups.

IDVH location	
ADMM	Number of dogs
T12-T13	2
T13-L1	1
L2-L3	3
L3-L4	1
L4-L5	2
FM	Number of dogs
T11-T12	1
T12-T13	4
T13-L1	2
L1-L2	3
L3-L4	3
L4-L5	2
L5-L6	1
L6-L7	1
Control group	Number of dogs
T11-T12	1
T12-T13	4
T13-L1	1
L1-L2	1
L2-L3	2
L3-L4	1

examined in any of the FM and control dogs. A T2\*-weighted GRE sequence was available in 8/9 dogs with ADMM, in 16/17 dogs with FM, and in all control dogs.

#### 3.3.1 | Signal Changes Dorsal to the Central Canal

In all nine dogs in the ADMM group, a dorsal intramedullary hypointense focus was observed on the transverse T2-weighted FSE sequence. In 8/9 ADMM dogs that had a T2\*-weighted GRE sequence available, a hypointense focus dorsal to the central canal was observed at the same location as observed on the T2-weighted FSE (100%; Figure 2 and [Supporting Information files](#)).

In the FM group, a hypointense signal dorsal to the central canal was visible in 8/17 dogs on transverse T2-weighted FSE images (47%; Figure 3). In 16/17 FM dogs, a T2\*-weighted gradient echo (GRE) was available. Of these 16 dogs, a hypointense focus on transverse T2\*-weighted GRE images was visible in three dogs (19%).

In control dogs, signal changes dorsal to the central canal were noted in 6/10 dogs in the T2-weighted FSE sequence (60%). In all



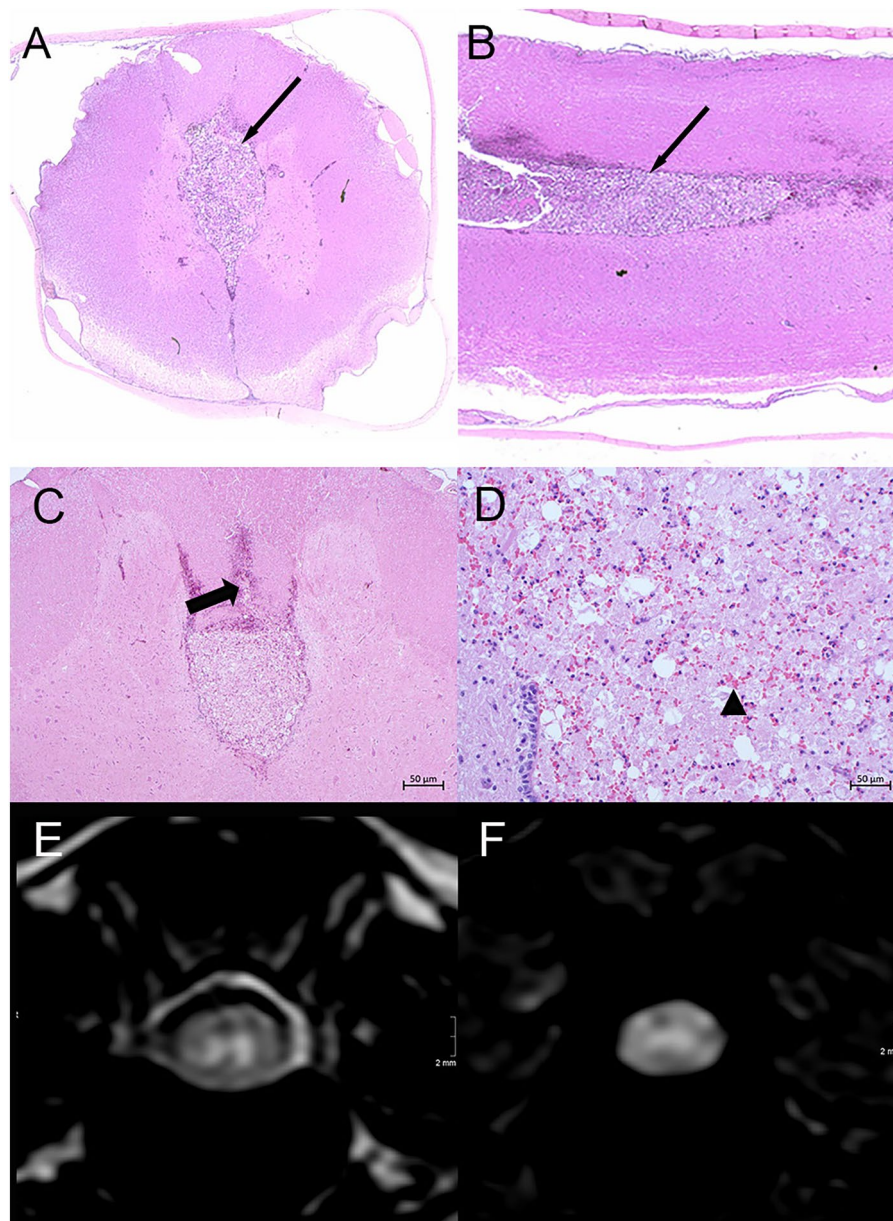


**FIGURE 1** | Spinal cord sections of a Chinese Crested dog (dog # 5), 3 years, intact male with ascending–descending myelomalacia (A) Cross section showing necrotic hemorrhagic debris in and dorsal of the central canal (arrow). (B) Longitudinal section showing the distended and ruptured central canal (arrow) over several segments. (C) Cross section of a segment far distant from the spinal cord injury. The central canal is distended and plugged with hemorrhagic necrotic spinal cord debris that is squeezed through the ruptured ependyma into the dorsal funiculus (arrow). (D) Higher magnification showing the vacuolized, hemorrhagic, and necrotic neuroparenchymatous plug (arrowhead) infiltrated by a few neutrophils. (E) T2-weighted fast spin echo and (F) T2\*-weighted gradient echo transverse images of the spinal cord demonstrating a faint hypointense signal dorsal to the central canal two vertebral body lengths caudal to the initial spinal cord injury.

control dogs, a T2\*-weighted GRE sequence was available and showed a mild hypointense focus in transverse T2\*-weighted GRE dorsal to the central canal in three of them (30%). A signal void interpreted as intramedullary hemorrhage was noted in 7/9 dogs with ADMM (78%) and in 5/17 dogs with FM (29%). No findings were interpreted as intramedullary hemorrhage in any of the control dogs.

No signal changes were observed on T1-weighted images in dogs with ADMM, FM, and control dogs. Table 3 presents the numbers of dogs in each group, the number of dogs for which a T2\*-weighted GRE sequence was available, the number of dogs

showing a hypointense signal dorsal to the central canal on T2\*-weighted GRE and T2-weighted fast spin echo sequences, and the number of dogs in which the signal alteration was interpreted as intramedullary hemorrhage.

### 3.3.2 | Length of Signal Changes

In dogs with ADMM, a T2-weighted hypointense focus dorsal to the central canal was visible on T2-weighted FSE images on 1–3 consecutive transverse images in 4/9 dogs, 3–5 consecutive transverse images in 4/9 dogs, and on > 5 consecutive images in

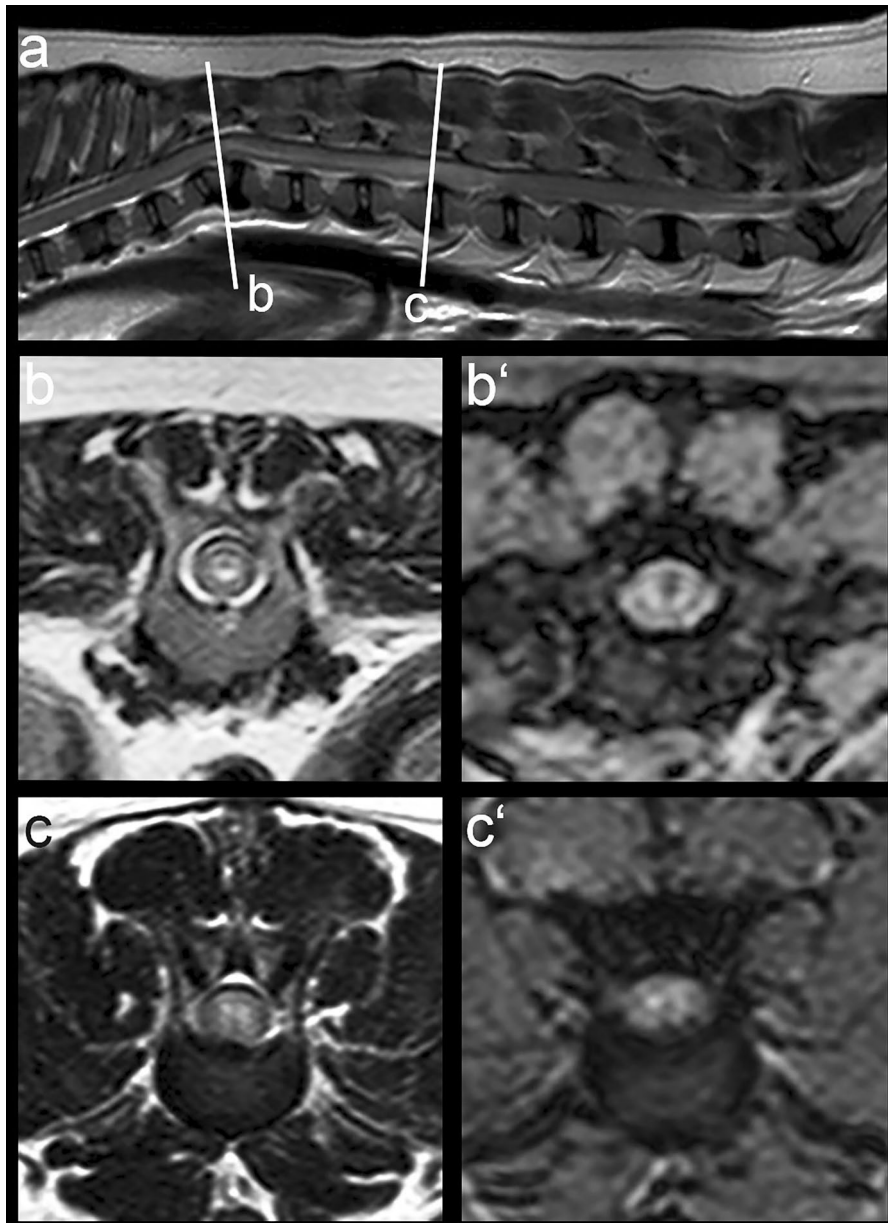


**FIGURE 2** | French Bulldog, 3 years, spayed female (dog # 9). T2-weighted sagittal image (a) of the lumbar spine diagnosed based on MRI as acute nucleus pulposus extrusion at L2/L3 (level c). Around three vertebral body lengths cranial to it (level b), an intramedullary hypointense focus slightly dorsal to the central canal was seen on T2-weighted fast spin echo and gradient echo sequence (c'). On transverse T2-weighted FSE (b) and transverse T2\* weighted gradient echo sequence (b') at the level of the spinal cord injury, the intramedullary signal is heterogeneously hyperintense. Euthanasia was performed on the same day of the MRI and pathology confirmed ascending and descending myelomalacia.

1/9 dogs. In one dog with ADMM, no transverse images were available caudal to the SCI.

Signal changes in dogs with FM were visible in 1–3 consecutive transverse images in 6/17 dogs, and in 4–5 consecutive transverse images in 2/17 dogs. The remaining nine dogs with FM did not have any signal changes dorsal to the central canal. No FM dog showed signal changes in > 5 consecutive transverse images.

In 5/10 control dogs, a T2-weighted hypointense focus dorsal to the central canal was seen on 1–3 consecutive images, whereas in 1 dog, changes were visible on 4 consecutive transverse images. However, in this latter dog, no hypointense focus was visible on

the transverse T2\*-weighted GRE sequence. The remaining four control dogs did not have any signal changes dorsal to the central canal. None of the control dogs had signal changes in > 5 consecutive transverse images.

### 3.3.3 | Distance of Signal Changes to the Initial SCI

The median distance of remote signal changes dorsal to the central canal in relation to the SCI was three times the length of a vertebral body (range, 2–6; IQR, 2.5–4.75) in dogs with ADMM. In dogs with FM, the distance of signal changes ranged from 0 to 2.5 vertebral body lengths, with a median of 0 (IQR, 0–1). The distance of the dorsal intramedullary signal changes to the SCI

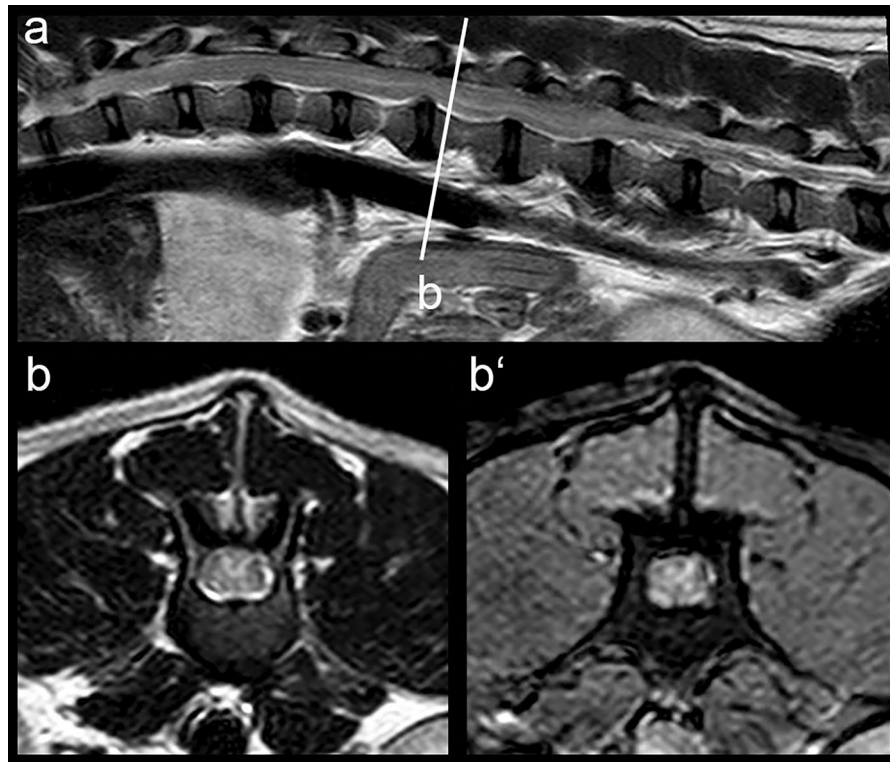


**FIGURE 3** | French Bulldog, 5 years, spayed female. T2-weighted sagittal image (a) of the lumbar spine diagnosed based on MRI as acute disc extrusion L5/L6 with extensive epidural hemorrhage. At the level of the cranial endplate of L3 (b) there is heterogeneous signal dorsal to the central canal with a hypointense center on T2-weighted fast spin echo (b) and a heterogeneous signal on T2\* weighted gradient echo sequence (b'). Euthanasia was performed on the same day of the MRI and pathology indicated focal myelomalacia without signs of ascending descending myelomalacia. This dog of the FM group was falsely categorized as ADMM based on the signal changes on MRI.

**TABLE 3** | Number of dogs in each group with T2\* weighted gradient echo (GRE) sequence available and with signal changes dorsal to the central canal in T2\* GRE and T2 weighted fast spin echo (FSE).

Group	Number of dogs	T2*-weighted GRE available	T2*-weighted GRE	T2-weighted FSE	Intramedullary hemorrhage
ADMM	9	8 (89%)	8 (100%)	9 (100%)	7 (78%)
FM	17	16 (94%)	3 (19%)	6 (35%)	5 (29%)
Control group	10	10 (100%)	3 (30%)	6 (60%)	0 (0%)

in the control group ranged from 0 to 1.5 vertebral body lengths, with a median of 0 (IQR, 0–1).

### 3.3.4 | Signal Changes Upon Follow-Up MRI Examinations

In the two dogs of the ADMM group with follow-up MRI examination, progression with increased lesion extent was observed: one dog had signal changes eight vertebral segments cranial from the SCI, and in the second dog, mild dorsal intramedullary T2-weighted hypointense signal changes were observed in the cervical spinal cord (Figure 4 and [Supporting Information files](#)).

Four of seventeen dogs with FM had follow-up MRI performed. In two of four dogs with FM, focal signal changes dorsal to the central canal were seen two and three vertebral bodies caudal

to the SCI in the follow-up MRI that were not noted on the first MRI. However, signal changes were not clearly confirmed on T2\*-weighted GRE images. In the other two dogs, no signal changes were noted dorsal to the central canal, which was unchanged from the first MRI examination. The location and extent of dorsal intramedullary T2-weighted focal hypointense signal changes are represented in the schematic drawings in the [Supporting Information files](#).

### 3.3.5 | Suppression of CSF Signal

A single shot turbo spin-echo sequence was available in 7/9 ADMM dogs. The CSF to L2 ratio was calculated in five dogs; in two dogs, no ratio could be measured because of complete attenuation along the entire spine. The mean ratio of the five dogs was 10.65 (median, 9.7; range, 6.5–15.65). In the FM group, a single shot turbo spin-echo sequence was available in 15 dogs;



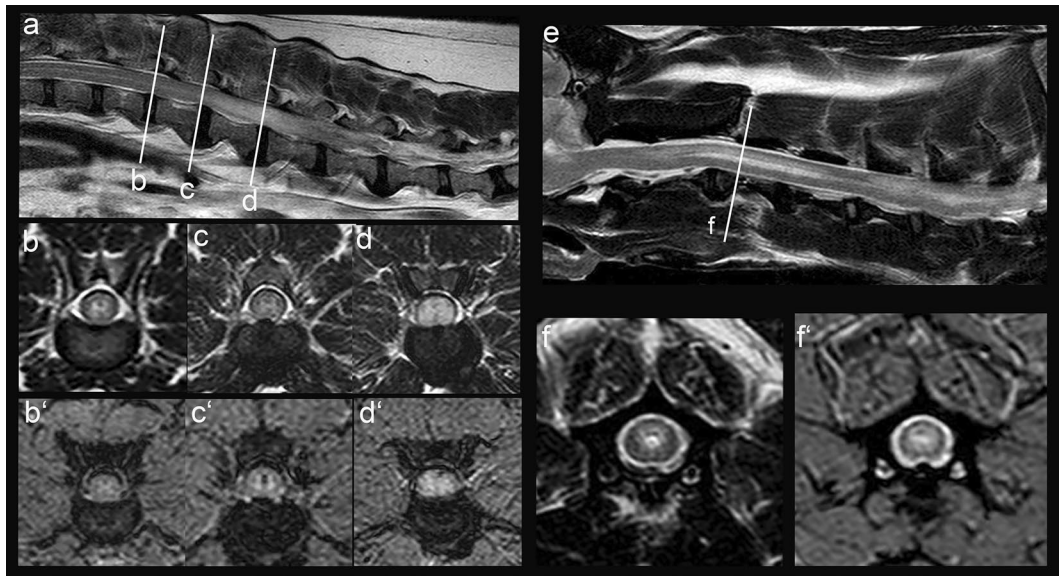


**FIGURE 4** | French Bulldog, 7years, spayed female (dog #7). T2-weighted sagittal image (a) of the lumbar spine diagnosed based on MRI as acute disc extrusion L3/L4 with and epidural hemorrhage caudal to it. There is increased intramedullary signal intensity visible on the sagittal images as well as heterogeneously increased signal intensity on transverse T2-weighted fast spin echo (d) and transverse T2\* weighted gradient echo images (d') with a focal intramedullary signal void indicating intramedullary hemorrhage. One vertebral body length cranial to the spinal cord injury (level c), a focal signal void is noted centrally within the spinal cord on the T2\*-weighted gradient echo image (c'), but not evident on T2-weighted fast spin echo (c). Two vertebral body lengths cranial to the spinal cord injury (level b), a focal T2-weighted hypointensity is seen on both, T2-weighted fast spin echo (b) and gradient echo (b'), that is located slightly dorsal to the center of the spinal cord. An MRI 6 days later showed extensive signal changes in the lumbar spine and a widened irregular central canal dilation in the cervical spine (e). The transverse images at level (f) show a mild hypointense signal dorsal to the widened central canal on both, T2-weighted fast spin echo image (f) and T2\*-gradient echo (f'). Pathology performed on the same day of the second MRI confirmed ascending and descending myelomalacia.

the mean ratio was 8.65 (median, 9.1; range, 0.6–20.13; IQR, 10.46–5.79). A single shot turbo spin-echo sequence was available in 7/10 control dogs, and the mean ratio was 4.84 (median, 2.85; range, 1.7–10.4; IQR, 7.99–2.45).

### 3.4 | Statistical Analysis

A comparison of the ADMM and control groups showed that the presence of a focal hypointense signal dorsal to the central canal on both T2-weighted FSE and T2\*-weighted GRE was significantly associated with ADMM ( $p=0.004$ ). Comparing the ADMM group with the FM group, the presence of signal changes in T2-weighted FSE and T2\*-weighted GRE images at a distance of  $\geq 2$  times the length of a vertebral body remote to the SCI was highly associated with ADMM ( $p < 0.001$ ). Overall, the presence of a T2-weighted hypointense signal dorsal to the central canal at a distance of  $> 3$  times the length of vertebral bodies remote to the SCI was highly associated with ADMM ( $p=0.01$ ).

The detection of a hypointense signal dorsal to the central canal based only on T2-weighted FSE sequences had a sensitivity of 100% for ADMM, with a specificity of 48%. The detection of an intramedullary hypointense signal dorsal to the central canal based on T2\*-weighted GRE had a sensitivity of 100% and a specificity of 73% for ADMM. Taking both T2-weighted sequences into account, the specificity for ADMM increased to 81%, whereas the sensitivity remained 100%. The detection of intramedullary signal changes dorsal to the central canal  $\geq 3$

vertebral body lengths in both T2-weighted sequences increased the specificity for ADMM to 100% but lowered the sensitivity to 78% (Table 4).

## 4 | Discussion

The presence of necrotic-hemorrhagic material inside and dorsal to the central canal even in remote spinal cord segments (at least three spinal cord segments) distant from the epicenter is a specific histological feature of ADMM and might play an important role in the longitudinal extension of hemorrhagic malacia within the spinal cord together with other biochemical and biomechanical mechanisms [2]. In comparison to ADMM, FM tends to be self-limiting, but lesion progression caused by disease dynamics cannot be ruled out.

Our aim was to identify histopathological features typical for ADMM on MRI of dogs with ADMM and compare these MRI features to those of dogs with histopathologically confirmed FM and with control dogs with severe SCI that recovered at least to non-ambulatory paraparesis. On MRI, signal heterogeneity dorsal to the central canal that resembled the histopathological changes in shape was observed, indicating necrotic-hemorrhagic material that was squeezed out of the central canal through a ruptured ependymal layer between the dorsal funiculi. The signal changes were heterogeneous, comprising a hypointense focus on T2-weighted FSE, T2\*-weighted GRE images, or both.



**TABLE 4** | Specificity and sensitivity of the prresence of a hypointense signal dorsal to the central canal.

	Sequence	Specificity (95% CI)	Sensitivity (95% CI)
Presence of a hypointense signal dorsal to the central canal	T2-weighted	48% (46–49)	100% (100)
	T2*-weighted	73% (72–74)	100% (100)
	T2 + T2*-weighted	81% (80–81)	100% (100)
≥ 3 vertebral body lengths	T2 + T2*-weighted	100% (100)	78% (77–79)

This MRI finding could represent the necrotic-hemorrhagic material found on histopathology dorsal to the central canal between the dorsal funiculi. However, focal signal changes also were present in T2-weighted FSE images in several dogs with FM and even in some control dogs that potentially could have FM associated with disc disease but that were not histologically evaluated because of clinical recovery.

Although the hypointense focus seen in T2-weighted FSE sequences correlated with the presence of a hypointense focus in T2\*-weighted sequences in all ADMM dogs in which a T2\*-weighted GRE sequence was available for interpretation, its presence on T2\*-weighted GRE was not a consistent finding in FM and control dogs, which seems to be an important difference among dogs with ADMM, FM, and control dogs. Therefore, the combination of a hypointense focus in T2\*-weighted GRE sequence and in T2-weighted FSE sequence was particularly helpful in our study using a 1.0 T magnet.

A T2-weighted FSE hypointensity on its own seemed to be subjective because it was sometimes difficult to differentiate abnormal hypointensity from the expected hypointense area between the gray matter. Semi-automatic image classification might be useful to minimize observer bias, but this method is not yet established in the clinical evaluation of MRI [20, 21]. Furthermore, the signal might be influenced by sequence parameters, the magnet used, coils, and field strength, and a generalization from our results might not be appropriate.

However, signal changes in the dorsal spinal cord distant from a SCI seem important because signal alterations > 3 vertebral segments distant from the SCI occurred only in dogs with ADMM. Observing signal changes in lesions distant from the site of SCI likely represents the longitudinal extension of ADMM identified in histopathology [2].

In contrast to the distance of the signal changes in remote spinal cord regions from the SCI, the length of signal changes themselves was not a reliable criterion to differentiate between groups. Concerning the differences between the ADMM and FM groups, overlap in the presence and length of a dorsal intramedullary T2-weighted hypointense focus was observed. This overlap might be partly explained by limitations arising from the group designation. In some dogs, progression from FM to ADMM was suspected based on a mismatch in location between histopathological findings and MRI. This mismatch could be explained by the delay between MRI examination and histopathology in some of the dogs. Such difficulties could be overcome by a prospective study design using a consistent MRI protocol

including larger areas of the spinal cord and T2\*-weighted GRE sequences in all dogs. Possibly, higher field strength and high-resolution sequences such as GRE T2-weighted images with isotropic voxels or susceptibility-weighted sequences also could be advantageous. Such prospective studies with blinded observers would be valuable to better understand the prognostic relevance of the observed dorsal intramedullary T2-weighted hypointense signal changes. However, it is challenging to identify sufficient dogs for prospective studies because of the low incidence of ADMM in dogs with SCI, which is <10% of dogs with SCI [4, 5, 16].

All but one dog with ADMM had MRI features of intramedullary hemorrhage, whereas such features were less often observed (5/17) in dogs with FM. Hemorrhage indicates a contusive type of the SCI and plays an important role in the progression of ADMM [2, 18]. Detection of intramedullary hemorrhage within the spinal cord seems to be of prognostic importance, and hence it would be of value to include GRE sequences or susceptibility-weighted sequences in the examination protocol in dogs with SCI.

Similar to a previous study [17], our mean CSF:L2 SSTSE attenuation values were higher in dogs with ADMM and FM (10.65 and 8.45, respectively) compared with control dogs (4.19). However, a recently proposed cut-off value of >7.4 [6, 17] also would include dogs with FM that possibly could recover. Nevertheless, we cannot rule out that dogs with FM also could encounter lesion progression to ADMM because of the highly dynamic nature of this disease.

In our study, a higher frequency of ADMM in French Bulldogs (36%) was seen in comparison to other breeds, but the small group sizes do not allow conclusions to be drawn about the overrepresentation of this breed in the ADMM group, and a possible association of ADMM and breed or epidural hemorrhage might be explored in future studies.

Our study had several limitations, most importantly its retrospective design because not all dogs had a T2\*-weighted GRE sequence and sequences distal or cranial to the observed signal changes available. A further limitation is that lesion detection of signal changes inside and dorsal to the central canal might be highly dependent on the magnetic field strength of the MRI scanner and therefore might lack reproducibility depending on the equipment available. Also, necropsy was performed with variable time delays after MRI examinations. Although a dorsal intramedullary T2-weighted hypointense signal dorsal to the central canal was visible in all dogs with ADMM, advanced

propagation or additional severe necrotic-hemorrhagic changes, or both, might have been observed on histopathology but might not yet have existed on MRI assessment. In addition, few follow-up MRI examinations and few MR images of the cervical spine were available to assess possible disease progression. Another major limitation is that the associations reported here were derived from preplanned statistical analyses. The small case numbers might limit the statistical power of these findings, and caution is advised because the findings might not be fully reproducible in larger populations with more breed diversity. Larger case numbers can help minimize the risk of breed bias and might either include more diversity of the breed population or confirm the higher frequency of ADMM in French Bulldogs, as observed in our study. A study design with larger group sizes, a consistent MRI protocol including larger areas of the spinal cord, possibly also of the cervical spine when ADMM is suspected, sequences sensitive to detect intramedullary hemorrhage, and follow-up MRI examinations should be included in future studies.

## 5 | Conclusion

In conclusion, we have described changes in and dorsal to the central canal on MRI that correlate with necrotic hemorrhagic material found in dogs with ADMM distant to the SCI. Based on these results, T2-weighted hypointense intramedullary signal changes at a distance  $\geq 3$  spinal segments remote from the SCI on T2-weighted FSE and T2\*-weighted GRE sequences might provide valuable information in providing an earlier diagnosis of ADMM and implying a poor prognosis. However, the presence of these signal changes on transverse T2-weighted FSE and transverse T2\*-weighted GRE images should not be used to support a recommendation for euthanasia. Instead, it might be viewed as an additional criterion for the development of ADMM. Additional multicenter prospective studies are essential to investigate a higher number of dogs and clarify the prognostic value of the observed MRI changes.

## Disclosure

The authors declare no off-label use of antimicrobials.

## Ethics Statement

The authors declare no Institutional Animal Care and Use Committee or other approval was needed. Authors declare human ethics approval was not needed.

## Conflicts of Interest

The authors declare no conflicts of interest.

## References

1. A. de Lahunta and E. Glass, "Lower Motor Neuron: Spinal Nerve, General Somatic Efferent System," In *Veterinary Neuroanatomy and Clinical Neurology*, 3rd ed. ed. A. de Lahunta and E. Glass. (W.B. Saunders, 2009), 77–133.
2. D. Henke, D. Gorgas, M. G. Doherr, J. Howard, F. Forterre, and M. Vandevelde, "Longitudinal Extension of Myelomalacia by Intramedullary

and Subdural Hemorrhage in a Canine Model of Spinal Cord Injury," *Spine Journal* 16, no. 1 (2016): 82–90.

3. M. Vandevelde, R. J. Higgins, and A. Oevermann, "General neuropathology," In *Veterinary Neuropathology: Essentials of Theory and Practice*, 1st ed. ed. M. Vandevelde, R. J. Higgins, and A. Oevermann (Wiley-Blackwell, 2012), 83–88.

4. J. M. Fingerroth and A. de Lahunta, "Ascending/Descending Myelomalacia Secondary to Intervertebral Disc Herniation," in *Advances in Intervertebral Disc Disease in Dogs and Cats*, 1st ed., ed. J. M. Fingerroth and W. B. Thomas (Wiley-Blackwell, 2015), 115–120.

5. N. Olby, "Current Concepts in the Management of Acute Spinal Cord Injury," *Journal of Veterinary Internal Medicine* 13, no. 5 (1999): 399–407.

6. A. Castel, N. J. Olby, C. L. Mariani, K. R. Muñana, and P. J. Early, "Clinical Characteristics of Dogs With Progressive Myelomalacia Following Acute Intervertebral Disc Extrusion," *Journal of Veterinary Internal Medicine* 31 (2017): 1782–1789.

7. P. Amsellem, J. Toombs, P. Laverty, et al., "Loss of Deep Pain Sensation Following Thoracolumbar Intervertebral Disk Herniation in Dogs: Treatment and Prognosis," *Compendium on Continuing Education for the Practicing Veterinarian* 25, no. 4 (2003): 266–274.

8. S. R. Platt, J. F. McConnell, and M. Bestbier, "Magnetic Resonance Imaging Characteristics of Ascending Hemorrhagic Myelomalacia in a Dog," *Veterinary Radiology & Ultrasound* 47, no. 1 (2006): 78–82.

9. D. Schweizer-Gorgas, "Ischemic Myelopathy, Spinal Cord Hemorrhage, Myelomalacia," in *Diagnostic MRI in Dogs and Cats*, 1st ed. ed. W. Mai (CRC Press, 2018), 565–583.

10. D. Lu, C. R. Lamb, and M. P. Targett, "Results of Myelography in Seven Dogs With Myelomalacia," *Veterinary Radiology & Ultrasound* 43, no. 4 (2022): 326–330.

11. N. Olby, J. Levine, T. Harris, K. Muñana, T. Skeen, and N. Sharp, "Long-Term Functional Outcome of Dogs With Severe Injuries of the Thoracolumbar Spinal Cord: 87 Cases (1996–2001)," *Journal of the American Veterinary Medical Association* 222, no. 6 (2003): 762–769.

12. F. Balducci, S. Canal, B. Contiero, and M. Bernardini, "Prevalence and Risk Factors for Presumptive Ascending/Descending Myelomalacia in Dogs After Thoracolumbar Intervertebral Disk Herniation," *Journal of Veterinary Internal Medicine* 31, no. 2 (2017): 498–504.

13. I. R. Griffiths, "Some Aspects of the Pathology and Pathogenesis of the Myelopathy Caused by Disc Protrusions in the Dog," *Journal of Neurology, Neurosurgery, and Psychiatry* 35, no. 3 (1972): 403–413.

14. A. Marquis, R. A. Packer, R. B. Borgens, and B. S. Duerstock, "Increase in Oxidative Stress Biomarkers in Dogs With Ascending–Descending Myelomalacia Following Spinal Cord Injury," *Journal of the Neurological Sciences* 353, no. 1 (2015): 63–69.

15. K. J. Cordle, G. S. Seiler, D. Barnes, et al., "MRI Features Can Help to Confirm a Diagnosis of Progressive Myelomalacia, but May Not Be Accurate in Dogs Lacking Characteristic Clinical Signs at the Time of Imaging," *Veterinary Radiology & Ultrasound* 64, no. 2 (2023): 283–293.

16. M. Okada, M. Kitagawa, D. Ito, T. Itou, K. Kanayama, and T. Sakai, "Magnetic Resonance Imaging Features and Clinical Signs Associated With Presumptive and Confirmed Progressive Myelomalacia in Dogs: 12 Cases (1997–2008)," *Journal of the American Veterinary Medical Association* 237, no. 10 (2010): 1160–1165.

17. L. J. Gilmour, N. D. Jeffery, K. Miles, and E. Riedesel, "Single-Shot Turbo Spin Echo Pulse Sequence Findings in Dogs With and Without Progressive Myelomalacia," *Veterinary Radiology & Ultrasound* 58, no. 2 (2017): 197–205.

18. D. Henke, M. Vandevelde, M. G. doherr, M. Stöckli, and F. Forterre, "Correlations Between Severity of Clinical Signs and Histopathological Changes in 60 Dogs With Spinal Cord Injury Associated With Acute

Thoracolumbar Intervertebral Disc Disease,” *Veterinary Journal* 198, no. 1 (2013): 70–75.

19. Y. Sato, S. Shimamura, T. Mashita, et al., “Serum Glial Fibrillary Acidic Protein as a Diagnostic Biomarker in Dogs With Progressive Myelomalacia,” *Journal of Veterinary Medical Science* 75, no. 7 (2013): 949–953.

20. E. Boudreau, A. Otamendi, J. Levine, J. F. Griffin, IV, L. Gilmour, and N. Jeffery, “Relationship Between Machine-Learning Image Classification of t2-Weighted Intramedullary Hypointensity on 3 Tesla Magnetic Resonance Imaging and Clinical Outcome in Dogs With Severe Spinal Cord Injury,” *Journal of Neurotrauma* 38, no. 6 (2021): 725–733.

21. E. Boudreau and N. Jeffery, “Semi- Automated Image Classification for Detection of T2 Hypointensity on 3T MRI in Dogs With Severe Spinal Cord Injury,” in Proceedings 32nd Symposium ESVN- ECVN Wroclaw, Poland 12th- 14th September 2019. *Journal of Veterinary Internal Medicine* 34 (2020): 2990–3057.

### **Supporting Information**

Additional supporting information can be found online in the Supporting Information section.